Nanoscale

COMMUNICATION

View Article Online
View Journal | View Issue

Cite this: *Nanoscale*, 2020, **12**, 10949

Received 17th January 2020,
Accepted 28th April 2020

DOI: 10.1039/d0nr00507j

rsc.li/nanoscale

Tunable wideband slot antennas based on printable graphene inks†

Xiaoxiao Chen,‡[a] Xu Liu,‡[b] Shouhao Li,[b] Weimin Wang,[a] Di Wei,*[b] Yongle Wu*[a] and Zhongfan Liu*[b,c,d]

Nano-materials could endow electronics with some new functionalities. A slot antenna with a tunable bandwidth, consisting of a planar slot antenna with graphene at the end and a gap located between the ground and a small patch, is proposed in this study. The printed graphene inks deposited onto the antenna are made of graphene powder and graphene oxide aqueous dispersion. Graphene oxide sheets function as effective surfactants providing assistance to form uniform inks; meanwhile, the tailored blending proportions endow the graphene inks with optimized original resistances. Dried graphene inks display alterable electrical resistance under DC voltages and the variation in the resistance affects the radiation of the antenna. The slot antenna realizes an operating bandwidth (reflection coefficient $|S_{11}| < -10$ dB) from 2.83 GHz to 6 GHz and a maximum frequency shift of 0.54 GHz after applying a DC voltage of less than 15 V. The graphene inks reported in this work integrate the dual advantages of graphene and graphene oxide. They not only provide stable and tunable graphene solution to antennas, but also could expand their applications in many other fields of electronic devices.

Introduction

Compared with 3G and 4G mobile communications, 5G mobile communication requires wider bandwidth, higher data rates, and more antennas than previous generations. With the wide applications and rapid development of wireless communication information systems and Internet of Things (IoT), the number of requirements in antenna design has increased. A highly integrated antenna with a tunable bandwidth and low energy consumption is urgently needed in order to simplify modules and adjust frequencies flexibly. Besides, tunable antenna technology can reduce the number and size of antennas and improve radio frequency (RF) performance, as a consequence, achieving better signal strength and higher speed signal transmission. Thus, it is meaningful to investigate tunable antennas. Frequency tunable antennas have been studied for a variety of practical applications, including mobile phones,[1] cognitive radio applications,[2] satellite applications[3] *etc*. By using PIN diodes,[4] varactors,[5] and microelectromechanical systems (MEMS),[6] electrically tunable antennas can be achieved. Recently, several kinds of new materials, such as liquid crystals,[7] liquid metals,[8] and ferrites,[9] have been introduced into tunable antennas. However, these tunable antennas have limited performances or require complicated manufacturing techniques.

Over 50 years of Moore's law, silicon is reaching its limits as a fundamental material in the electronics industry. Another element from the same family in the periodic table, carbon, is expected to start a new legend. In recent years, graphene has been researched extensively due to its extraordinary optical properties,[10] high electrical[11,12] and thermal conductivity,[13] and excellent mechanical properties.[14,15] Because of these characteristics, graphene has been reported as a promising material for wireless communication systems and components such as absorbers,[16,17] reflective cells,[18] antennas,[19–37] sensors,[38] phase-shifters,[39] filters,[40] attenuators,[41] and printable flexible electronics.[42] Compared with aforementioned materials, graphene can be easily manufactured and applied in devices. The electrical resistance of graphene could be simply changed by external electric fields, which alters the electrical characteristics of graphene-based microwave devices. Accordingly, graphene has great potential in various reconfigurable or tunable devices. In ref. 19–27 and 43, frequency tunable or reconfigurable antennas have been achieved.

[a]*School of Electronic Engineering, Beijing University of Posts and Telecommunications, Beijing 100876, China. E-mail: wuyongle138@gmail.com*
[b]*Beijing Graphene Institute, Beijing, China. E-mail: diwei@hotmail.com*
[c]*Beijing National Laboratory for Molecular Sciences, College of Chemistry and Molecular Engineering, Peking University, Beijing 100871, P. R. China. E-mail: zfliu@pku.edu.cn*
[d]*Center for Nanochemistry, Beijing Science and Engineering Center for Nanocarbons, P. R. China*

†Electronic supplementary information (ESI) available. See DOI: 10.1039/d0nr00507j

‡These authors contributed equally to this work.

However, most of the antennas[19–21,23,24] were presented only with theoretical analysis. Those with prototypes were either operated on narrow operating bandwidths[22,27,43] or displayed low frequency shifts.[25,26]

In this study, a tunable wideband slot antenna based on printable graphene inks is investigated. Different from the methods of applying bias voltage described in ref. 27 and 39, DC voltage is directly applied on the two ends of graphene, avoiding the design and use of bias circuits or tees. In our work, the printable graphene inks consist of graphene powder and graphene oxide (GO) sheets. Due to the reduction by a relatively low voltage of less than 15 V, the resistance of graphene decreases, providing a tuning effect on the operating bandwidth and frequency. In addition, the proposed antenna demonstrates the feasibility of achieving wideband with a relatively large frequency shift using only graphene-based materials. The proposed tunable wideband antenna is sufficient in common industrial applications, including RFID tags,[29,44] to manage inventory. Besides, the tunable antenna working as RFID reader antennas could be integrated in wearable monitoring systems to prevent the blinds from environmental damage.[45] Moreover, the wide bandwidth and directional radiation of the slot antenna could provide reliable and stable signal transmission between sensors and wearable devices for disease detection,[46] long-term health monitoring *etc*. Such cost-effective, easily acquired, and printable graphene inks could be further investigated in flexible tunable antennas and other printable electronic devices.

Results and discussion

Graphene powder and GO dispersion were purchased from Deyang Carbonene Technology Co., Ltd and Tanfeng Graphene Technology Co., Ltd, respectively. Graphene powder was first dispersed in deionized (DI) water by probe sonication (600 W, 1 h) without surfactants. Then the graphene inks were prepared by mixing graphene (5 mg ml^{-1}) and GO dispersion (5 mg ml^{-1}) in certain proportions followed by 1 h probe sonication. All the sonication processes were performed in an ice-bath, in order to avoid thermal reduction of GO. The ratios were further confirmed by the original resistances of graphene inks deposited on the antenna.

GO has been considered as surfactant sheets due to its hydrophilic edges and hydrophobic centers in the basal plane.[47,48] With the assistance of GO sheets, carbonaceous materials such as CNTs, C_{60}, and graphene could form uniform aqueous solutions. They could be successfully applied to specific application scenarios, such as highly conductive films of electromechanical sensors,[49] electrode materials for supercapacitors,[50] all-carbon solar cells,[51] active layers of photovoltaic devices *etc*.[52] In this work, GO was used as an effective binder to stabilize graphene sheets in water, forming graphene inks. Once the two types of carbon materials were mixed together in water, the oxygen groups on GO sheets functioned as a surfactant to allow strong interactions between graphene sheets. Besides, the π–π interaction between graphene and GO sheets also helped graphene powder to adsorb onto GO basal planes upon drying. Hence, this approach of realizing stable solution based on graphene inks can open a new application scenario in printable electronic devices.

The printable graphene inks were deposited onto the gap of the slot antenna, as shown in Fig. 1a. The design and simulations of the proposed antenna were carried out using an ANSYS HFSS full-wave simulator, in order to confirm the dimensions of each part in the slot antenna. The antenna consisted of a ground plane with the dried graphene ink (length: 3 mm) in the end of the slot and a microstrip feedline implemented on a Teflon substrate. The dielectric substrate with a dimension of 25 mm × 15 mm × 0.8 mm and a relative permittivity (ε_r) of 2.65 was processed. The thickness of the copper layer used in the ground plane and feeding line was 35 μm. An L-shaped gap was embedded on the ground, thus generating a rectangular patch in isolation with the ground to connect DC voltage. Details of the antenna design and the geometry of the proposed antenna are described in Fig. S1, S2 and Table S1.† Fig. 1b displays the simulated reflection coefficients for the antenna containing graphene with different resistances. According to the electromagnetic principle, the operating frequency and bandwidth of the slot antenna are related to the length and width of the slot. In this paper, the length (l_s) of the slot was set to be about a quarter wavelength of the operational center frequency. For the slot antenna, the imagin-

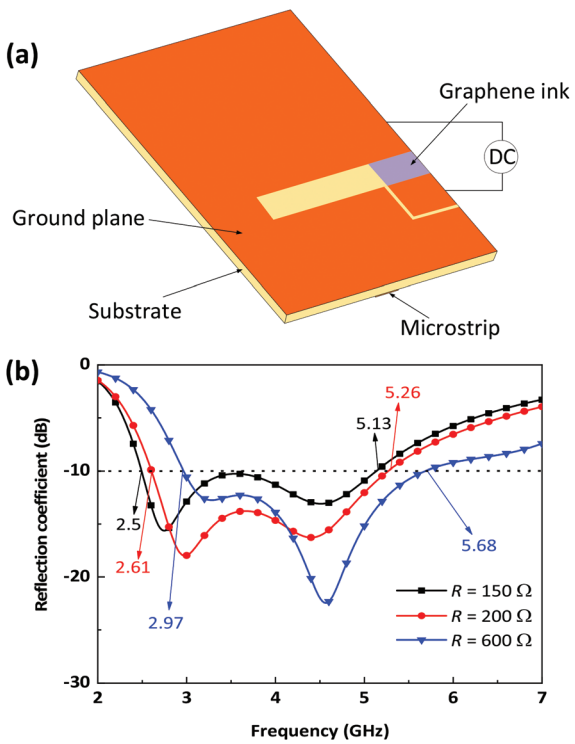

Fig. 1 (a) The structure of the proposed antenna. (b) Simulated reflection coefficients of the antenna containing dried graphene ink with a length of 3 mm under different resistances.

ary part of the input impedance shifts towards the inductive area with a decrease in the resistance, leading to the down-shift of the resonant frequency. In other words, the change in the resistance of graphene varies the equivalent length of the slot, which changes the operating bandwidth of the antenna.[27] Bias voltage was adopted in several literature studies to alter graphene resistances.[41] However, the bias circuit or bias tees will affect the electromagnetic performance of antennas, and also pose a great challenge to device miniaturization in real applications and increase the difficulty of circuit designs (Table S2†). Herein, DC voltage was directly applied to tune the resistances of graphene substituting for bias voltage, avoiding complex circuit design.

Optimizing the mixing ratio of graphene and GO, stable graphene inks could be obtained with appropriate resistances. Pure graphene powder had very low resistance (<20 Ω) on this antenna; GO was almost insulating and required a very high voltage to change its resistance. Thus, both graphene and GO couldn't function as ideal tunable resistors in tunable slot antenna applications. Fig. S5† displays the measured reflection coefficients of antennas based on graphene with different original resistances, which are obtained by different mixing ratios. The resistances were ~185 Ω, ~625 Ω, ~1240 Ω, and ~1480 Ω for the dried graphene inks mixed with ratios of 12 : 1, 10 : 1, 8 : 1, and 5 : 1 of graphene and GO.

Reflection coefficient measurements were performed using a vector network analyzer (VNA) as presented in Fig. 2a. At first, we used a source meter to apply DC voltage on graphene and removed it when stable resistances were attained. Then, a RF connector was attached to the antenna and the *S*-parameter could be recorded using a VNA. It is notable that the $|S_{11}|$ had no obvious change in large resistances, which was consistent with the simulated results shown in Fig. S4.† Therefore, the graphene ink with a ratio of 8 : 1 and an original resistance of ~625 Ω was chosen for further studies. After depositing graphene ink onto the slot, DC voltages (0–15 V) were directly applied and the resistance of the dried graphene ink decreased with increasing voltage. Here, three resistances of 625 Ω, 200 Ω, and 100 Ω were chosen for further characterization, corresponding to the applied DC voltages of 2 V, 13 V, and 15 V, respectively. DC voltages were removed after the dried graphene reached stable target resistances. Fig. 2b presents the measured reflection coefficients of the antenna with the decreased resistance. It can be seen that there was an obvious shift bandwidth at around 0.54 GHz from 6 GHz to 5.46 GHz in the upper band and almost no changes in the lower band. As expected, variations in the resistance of graphene modified the equivalent length of the slot, resulting in shifts in the resonance frequency of the antenna. When graphene resistance decreased, the resonance frequency presented a down-shift and further affected the operating bandwidth ($|S_{11}| < -10$ dB) of the slot antenna.

Raman spectroscopy (LabRAM HR Evolution) was used to characterize the carbon structure of graphene inks using a semiconductor laser (532 nm emission). The Raman spectra of GO, graphene powder, and graphene inks shown in Fig. 2c

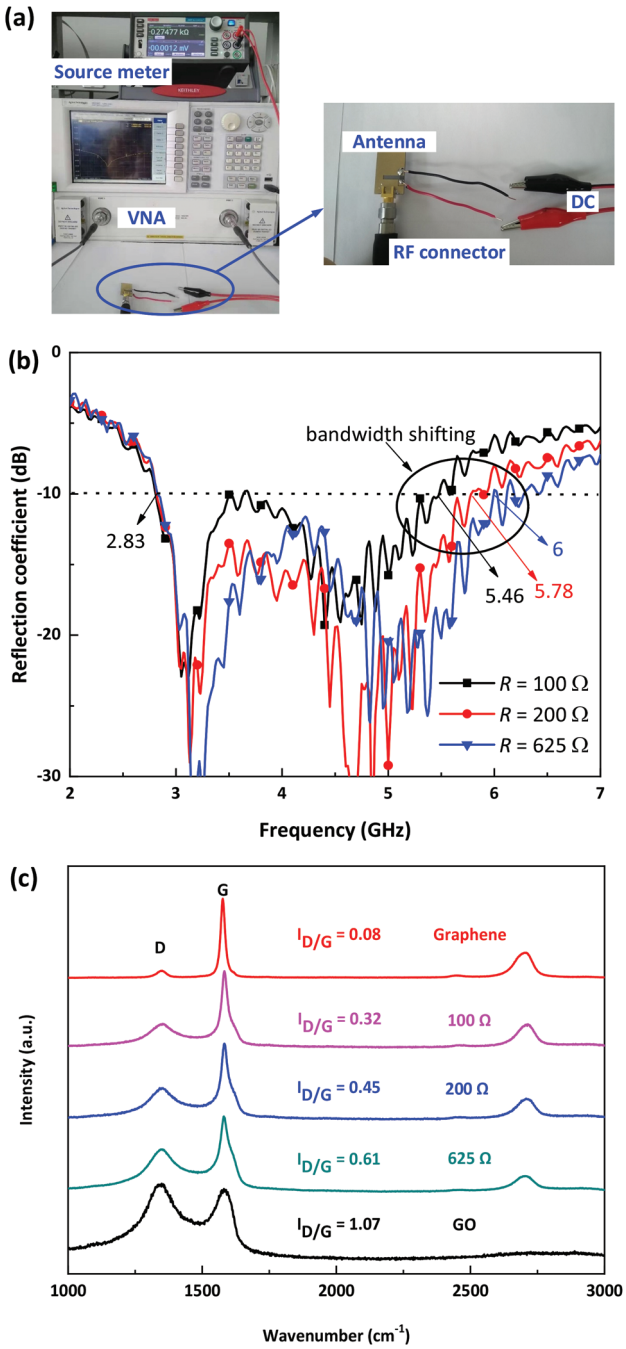

Fig. 2 (a) The measurement setup of the *S*-parameter. (b) Measured reflection coefficients *versus* frequency for the graphene ink with ~625 Ω resistance before and after applying DC voltages. (c) Raman spectra of GO, graphene ink, and graphene powder.

exhibit characteristic peaks, namely D-, G-, and 2D-band peaks at ~1350, ~1580, and ~2700 cm^{-1}, respectively. As shown in Fig. 2c, graphene powder presented a sharp G-band, a feeble D-band, and a wide 2D-band, confirming that the powder had a multi-layer graphene structure. The prominent D-band of GO was slightly higher than the G-band, indicating that the GO sheets consisted of abundant oxygen containing groups. Compared to graphene and GO, the Raman spectra of gra-

phene inks before and after application of DC voltages showed all the three feature peaks consistently. The G-band is active in sp^2-hybridized carbon-based materials, while the D-band is activated when the defects participate in the double resonance Raman scattering near the K point of the Brillouin zone. Therefore, the integrated intensity ratio $I_{D/G}$ of the D- to G-band is used to estimate the defect quantity in carbon structures.[53] The $I_{D/G}$ ratio of the original dried graphene ink was around 0.61, which was between the value of graphene and GO. The high $I_{D/G}$ ratio not only originated from the GO sheets, but also resulted from the fragmentation in graphene and GO sheets induced by probe sonication. The $I_{D/G}$ ratio decreased to 0.32 after applying DC voltages, manifesting that the gradual reduction attributed to the effect of the applied voltage effectively removed the oxygenated functional groups from the GO sheets.[54–57] Resulting from the rapid reduction under the DC voltage, the resistance of graphene ink decreased from ~625 Ω to ~100 Ω. The optical microscopy images of GO, graphene powder, and graphene inks obtained using an industrial microscope (LV100ND) are presented in Fig. S7.† A number of reduction methods can be used to tune the electrical resistance of GO, but they are not suitable for electronic devices. High temperature of thermal reduction[58] means large energy consumption and cannot be appropriate for GO films on substrates with a low melting-point. Chemical reduction[59] by reductants such as hydrazine,[60] $NaBH_4$,[61] ascorbic acid[62] or hydroiodic acid[63] may introduce impurities and residue, and the hazardous chemicals cannot be used on the device substrates. Electrochemical reduction[64] requires an electrophoresis device and buffer liquids. Obviously, DC voltage-induced reduction proposed in this paper is an energy-efficient and effective *ex situ* reduction method for GO used in the printed circuit board (PCB) of electronic devices.[65–67]

The measurements of far-field parameters, including gains, efficiencies, and radiation patterns, were carried out in a microwave anechoic chamber. The far-field performance of the antenna was measured in the microwave anechoic chamber as displayed in Fig. S3.† The antenna was connected with a RF connector in the turntable and fixed by tapes, and then the measurements were conducted by a Satimo system in the microwave anechoic chamber. Through processing the sampled signal received by the antenna in stargate, the system calculated all far-field performances. Fig. 3 depicts the measured boresight gains and efficiencies which are essential parameters for antennas. Gain refers to the ratio between the signal power density of the antenna and an ideal isotropic antenna along certain radiation directions. It quantificationally describes the radiation capacity of an antenna, which means that the reading distance increases with larger gain and it is directional. Efficiency is defined as the ratio of the radiated power to the input power of the antenna, and it is calculated by all the radiated (accepted) power of the antenna which is non-directional. The measured results revealed that the change in the resistance of graphene didn't vary the trend of gains and efficiency curves. It can be observed that the test outcomes were in line with the trend that both the gain and

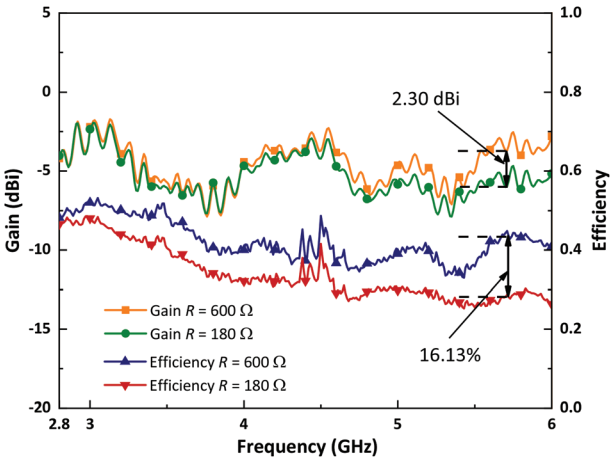

Fig. 3 Measured boresight gains and efficiencies of the antenna *versus* frequency at different resistances.

efficiency declined with the decreasing resistance, because graphene exhibited the lossy-dielectric behavior before the application of the voltage and moved towards the metallic behavior after applying the voltage.[43,68] The maximum variations in the gain and efficiency were about 2.30 dBi and 16.13%, respectively. Although the gain and efficiency of the antenna were reduced with decreasing resistance, the gains were larger than −7.87 dBi and efficiencies were higher than 25.24% over the whole operating bandwidth, satisfying with the original design that the gain must be larger than −11 dBi and the efficiency should be higher than 10%. Our design with a maximum gain of −1.7 dBi and an efficiency of 53% are capable of being used in sensor applications and RFID tags. In comparison with previous works, the proposed antenna has a higher efficiency, wider bandwidth, and tunability. Furthermore, the tunability over a wide band as well as the compact size of the antenna provide the possibility for minimization and integration of devices. The data of comparison are listed in Table 1.

Radiation patterns represent the strength of radio waves as a function of the angle in the far-field and they represent the radiation performance of an antenna in all directions. The radiation patterns were measured at 3 GHz in the planes of φ = 0° and φ = 90°, respectively, because the antenna exhibited the highest gain and efficiency around 3 GHz. By comparing the measurement (Fig. 4a) and simulation results (Fig. 4b), it can be observed that the addition of graphene didn't distort the general outline of the radiation patterns, and the differences were mainly due to environmental variations in the microwave anechoic chamber and the influence of repeated deposition. It is clearly noticed that the antenna presents different radiation strengths in distinct directions. In particular in the plane of φ = 0°, when the angle approached 90° or 270° the radiation strength sharply decreased so as hardly radiated energy outward. With the decrease in the graphene resistance, the amplitude of radiation patterns in the two planes declined, which was in accord with the trend of gain and efficiency shown in Fig. 3. From the illustration above, the application of

Table 1 Comparisons with other previous referenced prototypes based on graphene ink

Ref.	29	44	45	46	This work
Gain (dBi)	−2.18	−4	0.7	−0.6	−1.7
Efficiency	40%	32%	N. A.	N. A.	53%
Operating frequency/bandwidth	889 MHz	984–1052 MHz	2.4 GHz	0.89–1.02 GHz	2.83–6 GHz
Size (mm^2)	143 × 3	92 × 25	43 × 3	141.17 × 3.53	25 × 15
Tunability	No	No	No	No	Yes

N. A.: Not available.

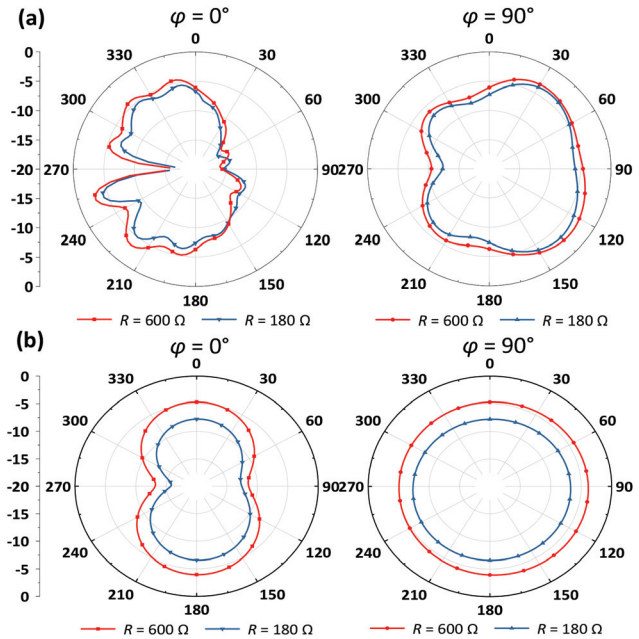

Fig. 4 (a) Measured and (b) simulated radiation patterns of the antenna at 3 GHz.

graphene in the slot antenna didn't deteriorate the overall performance of the antenna, but its resonance frequency and bandwidth was simply and effectively changed by external DC voltages. The proposed slot antenna offers a feasible scheme to design a tunable antenna integrated with graphene and can be extended into antenna arrays to further enhance gain and tunability.

Conclusions

A tunable wideband slot antenna based on printable graphene inks consisting of graphene powder and GO has been demonstrated in this letter. The GO here works as surfactant sheets conducting stable aqueous graphene inks without any supplementary surfactants, which may introduce further contaminants for electronic devices. Meanwhile, the original resistance of graphene inks can be simply adjusted by the blend ratios and concentrations of graphene-based materials. The cost-effective and easily achieved printable graphene inks open a new dimension in the field of printable wireless devices. By applying DC voltage on the dried graphene ink, the change in the resistance tunes the operating bandwidth of the slot antenna. The proposed antenna achieves a shifting bandwidth of 0.54 GHz from 6 GHz to 5.46 GHz. The measured results demonstrate the tunability of the operating bandwidth, and are in good agreement with the simulation results and verify the design concept. The tunable antenna implemented by simple DC voltages has been recognized as a promising approach to realize the miniaturization and highly integrated circuits for communication devices. Furthermore, it also enables great potential for wide applications of wireless flexible devices and printable electronics with low power consumption.

Conflicts of interest

There are no conflicts to declare.

Acknowledgements

This work was supported by the Beijing Municipal Science & Technology Commission (No. Z181100004818004, Z181100001018029, and Z191100006119027) and the Beijing Natural Science Foundation (No. JQ19018). The authors also appreciate the technical assistance from the BGI Characterization & Quality Assurance Center and the School of Electronic Engineering in Beijing University of Posts and Telecommunications.

Notes and references

1 Y. Li, Z. Zhang, J. Zheng, Z. Feng and M. F. Iskander, *IEEE Trans. Antennas Propag.*, 2012, **60**, 389–392.
2 Y. Cai, Y. J. Guo and T. S. Bird, *IEEE Trans. Antennas Propag.*, 2012, **60**, 2905–2912.
3 M. Ali, A. T. M. Sayem and V. K. Kunda, *IEEE Trans. Antennas Propag.*, 2007, **56**, 426–435.
4 H. A. Majid, M. K. A. Rahim, M. R. Hamid, N. A. Murad and M. F. Ismail, *IEEE Antennas Wirel. Propag. Lett.*, 2013, **12**, 218–220.
5 H. Li, J. Xiong, Y. Yu and S. He, *IEEE Trans. Antennas Propag.*, 2010, **58**, 3725–3728.
6 A. Zohur, H. Mopidevi, D. Rodrigo, M. Unlu, L. Jofre and B. A. Cetiner, *IEEE Antennas Wirel. Propag. Lett.*, 2013, **12**, 72–75.

7 A. C. Polycarpou, M. A. Christou and N. C. Papanicolaou, *IEEE Trans. Antennas Propag.*, 2014, **62**, 4980–4987.
8 A. Dey, R. Guldiken and G. Mumcu, *IEEE Trans. Antennas Propag.*, 2016, **64**, 2572–2576.
9 L.-R. Tan, R.-X. Wu, C.-Y. Wang and Y. Poo, *IEEE Antennas Wirel. Propag. Lett.*, 2013, **12**, 273–275.
10 R. R. Nair, P. Blake, A. N. Grigorenko, K. S. Novoselov, T. J. Booth, T. Stauber, N. M. R. Peres and A. K. Geim, *Science*, 2008, **302**, 1308–1309.
11 K. I. Bolotin, K. J. Sikes, Z. Jiang, M. Klim, G. Fudenberg, J. Hone, P. Kim and H. L. Stormer, *Solid State Commun.*, 2008, **146**, 351–355.
12 Z.-S. Wu, W. Ren, L. Gao, J. Zhao, Z. Chen, B. Liu, D. Tang, B. Yu, C. Jiang and H.-M. Cheng, *ACS Nano*, 2009, **3**, 411–417.
13 A. A. Balandin, S. Ghosh, W. Bao, I. Calizo, D. Teweldebrhan, F. Miao and C. N. Lau, *Nano Lett.*, 2008, **8**, 902–907.
14 M. Dragoman, D. Neculoiu, D. Dragoman, G. Deligeorgis, G. Konstantinidis, A. Cismaru, F. Coccetti and R. Plana, *IEEE Microw. Mag.*, 2010, **11**, 81–86.
15 C. Lee, X. Wei, J. W. Kysar and J. Hone, *Science*, 2008, **321**, 385–388.
16 M. Olszewska-Placha, B. Salski, D. Janczak, P. Ajurko, W. Gwarek and M. Jakubowska, *IEEE Trans. Antennas Propag.*, 2015, **63**, 565–572.
17 L. Ye, F. Zeng, Y. Zhang, X. Xu, X. Yang and Q. H. Liu, *Nanomaterials*, 2018, **8**, 834–844.
18 E. Carrasco, M. Tamagnone and J. Perruisseau-Carriera, *Appl. Phys. Lett.*, 2013, **102**, 1041103.
19 M. Tamagnone, J. S. Gómez-Díaz, J. R. Mosig and J. Perruisseau-Carrier, *Appl. Phys. Lett.*, 2012, **101**, 214102.
20 C. N. Alvarez, R. Cheung and J. S. Thompson, 2014 Loughborough Antennas and Propagation Conference, 2014, pp. 434–438.
21 T. Leng, X. Huang, X. Zhang and Z. Hu, 2015 IEEE 4th Asia-Pacific Conference on Antennas and Propagation, 2015, pp. 138–139.
22 J. Kumar, B. Basu, F. A. Talukdar and A. Nandi, 2017 IEEE MTT-S International Microwave and RF Conference, 2017, pp. 55–58.
23 A. A. A. Aziz, M. A. Abdalla and A. A. Ibrahim, 2018 International Symposium on Antennas and Propagation, 2018, pp. 471–472.
24 Y. Luo, Q. Zeng, X. Yan, Y. Wu, Q. Lu, C. Zheng, N. Hu, W. Xie and X. Zhang, *IEEE Access*, 2019, 30802.
25 M. Dragoman, D. Neculoiu, A.-C. Bunea, G. Deligeorgis, M. Aldrigo, D. Vasilache, A. Dinescu, G. Konstantinidis, D. Mencarelli, L. Pierantoni and M. Modreanu, *Appl. Phys. Lett.*, 2015, **106**, 153101.
26 A.-C. Bunea, D. Neculoiu, M. Dragoman, G. Konstantinidis and G. Deligeorgis, Proceedings of the 45th European Microwave Conference, 2015, pp. 614–617.
27 M. Yasir, P. Savi, S. Bistarelli, A. Cataldo, M. Bozzi, L. Perregrini and S. Bellucci, *IEEE Antennas Wirel. Propag. Lett.*, 2017, **16**, 2380–2383.
28 M. M. Mansor, S. K. A. Rahim and U. Hashim, 2014 International Symposium on Technology Management and Emerging Technologies, 2014, pp. 29–33.
29 M. Akbari, M. W. A. Khan, M. Hasani, T. Björninen, L. Sydänheimo and L. Ukkonen, *IEEE Antennas Wirel. Propag. Lett.*, 2016, **15**, 1569–1572.
30 P. Kopyt, B. Salski, M. Olszewska-Placha, D. Janczak, M. Sloma, T. Kurkus, M. Jakubowska and W. Gwarek, *IEEE Trans. Antennas Propag.*, 2016, **64**, 2862–2868.
31 S. Kosuga, R. Suga, O. Hashimoto and S. Koh, *Appl. Phys. Lett.*, 2017, **110**, 233102.
32 N. M. Jizat, S. N. Mohamad and M. I. Ishak, 3rd Electronic and Green Materials International Conference 2017, 2017, vol. **1885**, p. 020126.
33 J. Kumar, B. Basu, F. A. Talukdar and A. Nandi, *J. Electromagnet. Wave.*, 2017, **31**, 2046–2054.
34 J. Kumar, B. Basu, F. A. Talukdar and A. Nandi, *IEEE Antennas Wirel. Propag. Lett.*, 2018, **17**, 1861–1866.
35 R. Song, G.-L. Huang, C. Liu, N. Zhang, J. Zhang, C. Liu, Z. P. Wu and D. He, *Int. J. RF Microw. C. E.*, 2019, **29**, e21692.
36 H. Qiu, H. Liu, X. Jia, X. Liu, Y. Li, T. Jiang, B. Xiong, Y. Yang and T.-L. Ren, *RSC Adv.*, 2018, **8**, 37534–37539.
37 M. Yasir, M. Aldrigo, M. Dragoman, A. Dinescu, M. Bozzi, S. Iordanescu and D. Vasilache, *IEEE Electron Device Lett.*, 2019, **40**, 628–631.
38 B. Wu, X. Zhang, B. Huang, Y. Zhao, C. Cheng and H. Chen, *Sensors*, 2017, **17**, 2070.
39 M. Yasir, S. Bistarelli, A. Cataldo, M. Bozzi, L. Perregrini and S. Bellucci, *IEEE Microw. Wirel. Compon. Lett.*, 2019, **29**, 47–49.
40 D. Correas-Serrano, J. S. Gomez-Diaz, J. Perruisseau-Carrier and A. A. Lvarez-Melcón, *IEEE Trans. Nanotechnol.*, 2014, **13**, 1145–1153.
41 L. Pierantoni, D. Mencarelli, M. Bozzi, R. Moro, S. Moscato, L. Perregrini, F. Micciulla, A. Cataldo and S. Bellucci, *IEEE Trans. Antennas Propag.*, 2015, **63**, 2491–2497.
42 P. G. Karagiannidis, S. A. Hodge, L. Lombardi, F. Tomarchio, N. Decorde, S. Milana, I. Goykhman, Y. Su, S. V. Mesite, D. N. Johnstone, R. K. Leary, P. A. Midgley, N. M. Pugno, F. Torrisi and A. C. Ferrari, *ACS Nano*, 2017, **11**, 2742–2755.
43 M. Grande, G. V. Bianco, D. Laneve, P. Capezzuto, V. Petruzzelli, M. Scalora, F. Prudenzano, G. Bruno and A. D'Orazio, *Appl. Phys. Lett.*, 2019, **115**, 133103.
44 T. Leng, X. Huang, K. Chang, J. Chen, M. A. Abdalla and Z. Hu, *IEEE Antennas Wirel. Propag. Lett.*, 2016, **15**, 1565–1568.
45 W. Wang, C. Ma, X. Zhang, J. Shen, N. Hanagata, J. Huangfu and M. Xu, *Sci. Technol. Adv. Mater.*, 2019, **20**, 870–875.
46 X. Huang, T. Leng, X. Zhang, J. C. Chen, K. H. Chang, A. K. Geim, K. S. Novoselov and Z. Hu, *Appl. Phys. Lett.*, 2015, **106**, 203105.
47 L. J. Cote, J. Kim, V. C. Tung, J. Luo, F. Kim and J. Huang, *IEEE Electron Device Lett.*, 2010, **83**, 95–110.

48 A. R. Koltonow, J. Kim, L. J. Cote, J. Luo and J. Huang, *Mater. Res. Soc. Symp. Proc.*, 2012, **1344**, 93–100.
49 T. T. Tung, J. Yoo, F. K. Alotaibi, M. J. Nine, R. Karunagaran, M. Krebsz, G. T. Nguyen, D. N. Tran, J. F. Feller and D. Losic, *ACS Appl. Mater. Interfaces*, 2016, **8**, 16521–16532.
50 S. H. Aboutalebi, A. T. Chidembo, M. Salari, K. Konstantinov, D. Wexler, H. K. Liu and S. X. Dou, *Energy Environ. Sci.*, 2011, **4**, 1855.
51 V. C. Tung, J.-H. Huang, J. Kim, A. J. Smith, C.-W. Chu and J. Huang, *Energy Environ. Sci.*, 2012, **5**, 7810.
52 V. C. Tung, J. H. Huang, I. Tevis, F. Kim, J. Kim, C. W. Chu, S. I. Stupp and J. Huang, *J. Am. Chem. Soc.*, 2011, **133**, 4940–4947.
53 M. A. Pimenta, G. Dresselhaus, M. S. Dresselhaus, L. G. Cancado, A. Jorioa and R. Saitoe, *Phys. Chem. Chem. Phys.*, 2007, **9**, 1276–1291.
54 X. Lin, X. Shen, Q. Zheng, N. Yousefi, L. Ye, Y.-W. Mai and J.-K. Kim, *ACS Nano*, 2012, **6**, 10708–10719.
55 X. Lin, X. Liu, J. Jia, X. Shen and J.-K. Kim, *Compos. Sci. Technol.*, 2014, **100**, 166–173.
56 O. Ö. Ekiz, M. Urel, H. Güner, A. K. Mizrak and A. Dâna, *ACS Nano*, 2011, **5**, 2475–2482.
57 S. Pei and H.-M. Cheng, *Carbon*, 2012, **50**, 3210–3228.
58 H. C. Schniepp, J.-L. Li, M. J. McAllister, H. Sai, M. Herrera-Alonso, D. H. Adamson, R. K. Prud'homme, R. Car, D. A. Saville and I. A. Aksay, *J. Phys. Chem. B*, 2006, **110**, 8535–8539.
59 S. Stankovich, D. A. Dikin, R. D. Piner, K. A. Kohlhaas, A. Kleinhammes, Y. Jia, Y. Wu, S. T. Nguyen and R. S. Ruoff, *Carbon*, 2007, **45**, 1558–1565.
60 C. Gómez-Navarro, R. T. Weitz, A. M. Bittner, M. Scolari, A. Mews, M. Burghard and K. Kern, *Nano Lett.*, 2007, **7**, 3499–3503.
61 H. J. Shin, K. K. Kim, A. Benayad, S. M. Yoon, H. K. Park, I. S. Jung, M. H. Jin, H. K. Jeong, J. M. Kim, J. Y. Choi and Y. H. Lee, *Adv. Funct. Mater.*, 2009, **19**, 1987–1992.
62 M. J. Fernández-Merino, L. Guardia, J. I. Paredes, S. Villar-Rodil, P. Soís-Fernández, A. Martínez-Alonso and J. M. D. Tascón, *J. Phys. Chem. C*, 2010, **114**, 6426–6432.
63 S. Pei, J. Zhao, J. Du, W. Ren and H.-M. Cheng, *Carbon*, 2010, **48**, 4466–4474.
64 S. J. An, Y. Zhu, S. HwaLee, M. D. Stoller, T. Emilsson, S. Park, A. Velamakanni, J. An and R. S. Ruoff, *J. Phys. Chem. Lett.*, 2010, **1**, 1259–1263.
65 A. Rani, J.-M. Song, M. J. Lee and J.-S. Lee, *Appl. Phys. Lett.*, 2012, **101**, 233308.
66 P. Yao, P. Chen, L. Jiang, H. Zhao, H. Zhu, D. Zhou, W. Hu, B.-H. Han and M. Liu, *Adv. Mater.*, 2010, **22**, 5008–5012.
67 X. Li, D. Zhang, P. Zhu and C. Yang, *Bull. Mater. Sci.*, 2014, **37**, 629–634.
68 B. Wu and Y. Hao, The 8th European Conference on Antennas and Propagation (EuCAP), 2014.